

## Non-Invasive (Real-Time) Imaging of Histologic Margin of a Proliferative Skin Lesion *In Vivo*

To the Editor:

Confocal microscopy is a technique for imaging thin sections with high contrast within an optically turbid object. The imaging is non-invasive and does not require preparation of sections (which is done for conventional microscopy or routine histology). In the last 10 y, confocal microscopy has been increasingly used in biology (Pawley, 1995). In the past 5 y, this technique has been applied for imaging human skin *in vivo* (New *et al* 1991; Corcuff and Leveque, 1993; Corcuff *et al* 1993; Bertrand and Corcuff, 1994; Rajadhyaksha *et al*, 1995). In 1995, we reported the ability to image nuclear- and cellular-level detail in human skin *in vivo* with a video-rate confocal scanning laser microscope (Rajadhyaksha *et al*, 1995). A video-rate (real-time) confocal scanning laser microscope was designed and constructed that provides, to the best of our knowledge, the highest resolution and speed of imaging of living human skin. Unlike routine histology and confocal fluorescence microscopy, imaging is without the use of stains, and thus probes tissue in its native state. Melanin is the best endogenous contrast source for confocal reflectance imaging in human skin. Imaging was with visible (400–700 nm) wavelengths that penetrated to the dermo-epidermal junction. Standard oil immersion objectives were used.

We have recently improved confocal scanning laser microscope performance with the use of deeper penetrating near-infrared wavelengths (800–1064 nm) and water immersion objective lenses of numerical aperture (NA) 0.7–1.2. Water is of refractive index 1.33 and closely matches the 1.34 of the living epidermis (Tearney *et al*, 1995); this reduces aberrations and minimizes loss of resolution and contrast when imaging deep in the skin. The refractive index of water does not match to the  $\approx 1.55$  of the stratum corneum, and this, of course, produces spherical aberration. The resolution and contrast in our images, however, suggest that this aberration may be small; this is probably because the stratum corneum is thin ( $\approx 10 \mu\text{m}$ ) compared with the  $\approx 100 \mu\text{m}$  thick epidermis. The diffraction-limited resolution depends on wavelength  $\lambda$  and objective lens NA: the lateral resolution is  $0.5\lambda/\text{NA}$  and the axial resolution (section thickness) is  $1.4n\lambda/\text{NA}^2$  (Pawley, 1995), where  $n$  is the refractive index of the immersion medium. With the 1064 nm wavelength and high NA lenses, we can thus image horizontal (en face) sections, measured to be 2–5  $\mu\text{m}$  thin, within living tissue with measured lateral resolution of 0.5–1.0  $\mu\text{m}$ , to a depth of 300–400  $\mu\text{m}$  in the reticular dermis. Our experimentally measured lateral resolution and axial resolution (section thickness) closely agree with the predicted diffraction-limited values. The confocal section thickness compares well with that of sections that are microtomed for routine histology. A mechanical fixture was developed for stable microscope-to-skin contact. The fixture kept the skin laterally stable to within  $\pm 25 \mu\text{m}$  ( $\pm$  two cells), and allowed imaging at various topographic sites (arms, legs, torso, back, face, forehead) on the human body.

Recently, we characterized the typical histologic features of psoriatic lesions with the confocal scanning laser microscope. These histologic findings are Munro's microabscesses, parakeratotic stratum corneum, increased ratio between thickness of suprapapillary epidermal

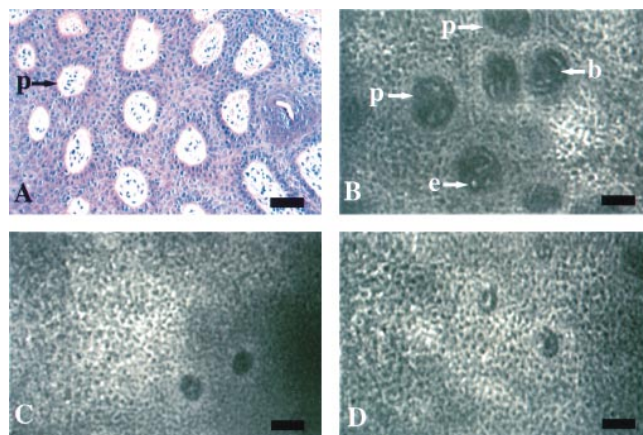


**Figure 1. Routine histology (A) correlates well with real-time confocal reflectance images (B) of a psoriatic lesion *in vivo*, obtained at the dermo-epidermal level.** The confocal images reveal significant morphologic differences between involved (B) and immediately adjacent uninvolved (C) skin. The major histologic characteristics that distinguish the uninvolved skin (C) from lesional psoriatic skin (B) are: (i) papillomatosis or increased number of papillae (p); (ii) enlargement of dermal blood vessels (b) supplying the proliferative lesion with circulating erythrocytes (e); and (iii) elongation of the epidermal rete ridges (González *et al*, unpublished data). The transitional skin (D) from uninvolved (C) to involved (B) skin was less than 400  $\mu\text{m}$  wide. Objective lens: 30 $\times$ , 0.9 NA water immersion, wavelength 1064 nm, measured lateral resolution 0.7  $\mu\text{m}$  and section thickness 3  $\mu\text{m}$ ; scale bar: 50  $\mu\text{m}$ .

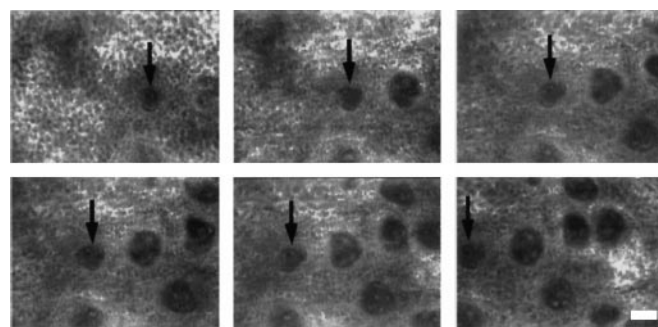


**Figure 2. Sequence of frames (grabbed from videotape) showing the increase in dermal papillae across the margin of a psoriatic lesion.** Arrow points to a specific papilla in the sequence. Scale bar: 50  $\mu\text{m}$ .

plates and elongated epidermal crests, and papillomatosis.<sup>1</sup> We show for the first time that we can confocally image the histologic margin of a proliferative skin lesion *in vivo*. We used a 30 $\times$ , 0.9 NA water immersion objective lens; the low magnification allows imaging of a large (530  $\mu\text{m}$ ) field of view whereas the high NA provides histology-like resolution that was measured to be 0.7  $\mu\text{m}$  (lateral) and 3  $\mu\text{m}$  (section thickness). **Figure 1** shows routine histology

Manuscript received March 3, 1998; revised April 30, 1998; accepted for publication May 13, 1998.

<sup>1</sup>González S, Rubinstein G, Rajadhyaksha M, White WM, González E, Anderson RR. Real-time confocal imaging of psoriasis *in vivo*. *Int Invest Dermatol* 657, 1998 (abstr.)

and confocal images of an oval, sharply marginated, erythematous psoriatic lesion, 9 mm in diameter located on the outer forearm. The images show lesional (involved) skin at the dermo-epidermal level, the border of the lesion, and immediately adjacent normal (uninvolved) skin. Papillomatosis (increased number and size of dermal papillae) is one major histologic feature of psoriasis; this was easily visualized in the confocal images. A series of frames from confocal images of the dermo-epidermal junction showing the transitional margin of a psoriatic lesion is presented in **Fig 2**.

This study suggests that potential applications of confocal reflectance microscopy include precise real-time detection of lesion margins *in vivo*. This may eventually lead to confocal imaging-guided surgeries including biopsies and Mohs' micrographic surgery.

Salvador González,\* Milind Rajadhyaksha,\*† and  
R. Rox Anderson\*

\*Wellman Laboratories of Photomedicine, Dermatology

Department, Massachusetts General Hospital, Harvard Medical  
School, Boston, Massachusetts, U.S.A.  
†Lucid, Henrietta, New York, New York, U.S.A.

#### REFERENCES

- Bertrand C, Corcuff P: *In Vivo* spatio-temporal visualization of the human skin by real-time confocal microscopy. *Scanning* 16:150-154, 1994
- Corcuff P, Leveque JL: *In Vivo* vision of the human skin with the tandem scanning microscope. *Dermatology* 186:50-54, 1993
- Corcuff P, Bertrand C, Leveque JL: Morphometry of human epidermis *in vivo* by real-time confocal microscopy. *Arch Dermatol Res* 285:475-481, 1993
- New KC, Petroll WM, Boyde A, et al: *In vivo* imaging of human teeth and skin using real-time confocal microscopy. *Scanning* 13:369-372, 1991
- Pawley JB: (ed.) *Handbook of Biological Confocal Microscopy*, 2nd edn. New York: Plenum Press, 1995
- Rajadhyaksha M, Grossman M, Esterowitz D, Webb RH, Anderson RR: *In vivo* confocal scanning laser microscopy of human skin; melanin provides strong contrast. *J Invest Dermatol* 104:946-952, 1995
- Tearney GJ, Brezinski ME, Southern JF, Bouma BE, Hee MR, Fujimoto JG: Determination of the refractive index of highly scattering human tissue by optical coherence tomography. *Optics Lett* 20:2258-2260, 1995

## Somatic Mutations of the MEN1 Tumor Suppressor Gene Detected in Sporadic Angiofibromas

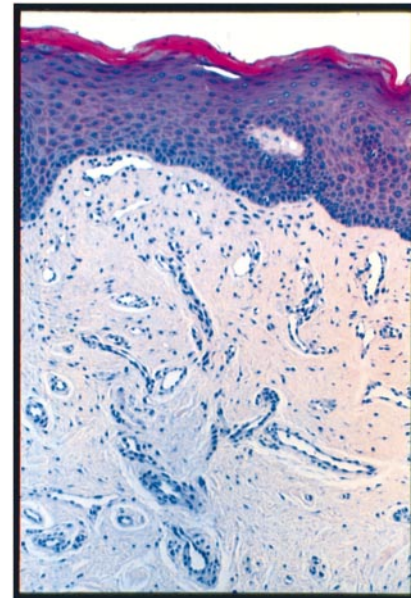
To the Editor:

Angiofibromas are benign cutaneous tumors that can occur sporadically or as multiple lesions in association with inherited diseases. Multiple facial angiofibromas were previously thought to be pathognomonic for tuberous sclerosis (Darling *et al*, 1997); however, it has recently been shown that angiofibromas may also be associated with multiple endocrine neoplasia type I (MEN1) (Darling *et al*, 1997). The genetic changes leading to the development of angiofibromas are unknown. The MEN1 gene has been recently mapped (Larsson *et al*, 1988) and identified (Chandrasekharappa *et al*, 1997). Tumors in MEN1 disease, including benign tumors of the parathyroid glands, pituitary glands, and pancreas, show genetic alterations of the MEN1 gene and the association of cutaneous angiofibromas with MEN1 disease was recently confirmed by genetic analysis (Pack *et al*, 1998). Because MEN1 gene alterations are involved in MEN1-associated angiofibromas, we decided to investigate whether MEN1 gene alterations can also be detected in sporadic angiofibromas. For this purpose, we analyzed 19 sporadic facial angiofibromas (**Fig 1**) for mutations in the MEN1 gene using polymerase chain reaction based SSCP and sequencing analysis. All patients had a negative family history for tuberous sclerosis and MEN1 disease.

Tumor tissue and adjacent normal control tissue was removed from histologic sections under light microscopic visualization, placed in DNA extraction buffer (50 mmol Tris-HCL per liter, 1 mmol ethylenediamine tetraacetate per liter, 0.5% Tween-20, and 0.5 mg proteinase K per ml, pH 8.0), and incubated overnight at 37°C, followed by thermal inactivation of proteinase K (95°C for 5 min).

Polymerase chain reaction/SSCP analysis was performed using 13 primer sets with designed intronic sequences to amplify the coding sequence of exons 2-10 of the MEN1 gene as previously described. Aberrant bands were identified in two of the 19 analyzed angiofibromas involving exons 2 (pt#3) and 8 (pt#5). The DNA from these two tumors was subjected to sequencing analysis.

Aberrant bands were detected in two tumors (**Fig 2**). The mutations consisted of a A→T transition at nucleotide 517 (AAG to TAG; K135I) and a transversion of GG→AA at nucleotide 1184-5 (GAG GAG to



H

**Figure 1.** Cutaneous angiofibroma (case 3) with dermal fibrosis and prominent vascular architecture. Scale bar: 100  $\mu$ m.

GAA AAG; E358E; E359K) on exons 2 and 8, respectively (**Fig 2**). The mutations were only observed in the tumor DNA, but not in the normal control tissue. LOH analysis was performed using two polymorphic markers flanking the gene on both sides (PYGM, D11S449, Research Genetics, Huntsville, AL). None of the 19 angiofibromas showed LOH, including the two sections displaying mutations.

Angiofibromas consist of at least two different types of proliferating cells, which have been referred to as vascular cells and spindle-shaped, triangular, or stellate cells of unknown origin (Lever and Schaumburg-Lever, 1990) (**Fig 1**). Therefore, angiofibromas may in fact consist of a mixed population of neoplastic and non-neoplastic cells, and LOH results may be obscured by "contamination" with normal somatic cells. Somatic cell "contamination" can be observed in our SSCP analysis in the two cases with mutations, which show marked wild-type bands and less intense aberrant bands (**Fig 2**). Similarly, "contamination"